Ab initio MRCI + Q study on potential energy curves and spectroscopic parameters of low-lying electronic states of CS^+*

Li Rui(李 瑞)[a)†], Wei Chang-Li(魏长立)[b)], Sun Qi-Xiang(孙启响)[b)], Sun Er-Ping(孙二平)[b)], Jin Ming-Xing(金明星)[b)], Xu Hai-Feng(徐海峰)[b)], and Yan Bing(闫 冰)[b)‡]

[a)] *Department of Physics, College of Science, Qiqihar University, Qiqihar* 161006, *China*
[b)] *Institute of Atomic and Molecular Physics, Jilin University, Changchun* 130012, *China*

(Received 14 March 2013; revised manuscript received 6 May 2013)

Carbon monosulfide molecular ion (CS^+), which plays an important role in various research fields, has long been attracting much interest. Because of the unstable and transient nature of CS^+, its electronic states have not been well investigated. In this paper, the electronic states of CS^+ are studied by employing the internally contracted multireference configuration interaction method, and taking into account relativistic effects (scalar plus spin–orbit coupling). The spin–orbit coupling effects are considered via the state-interacting method with the full Breit–Pauli Hamiltonian. The potential energy curves of 18 Λ–S states correlated with the two lowest dissociation limits of CS^+ molecular ion are calculated, and those of 10 lowest Ω states generated from the 6 lowest Λ–S states are also worked out. The spectroscopic constants of the bound states are evaluated, and they are in good agreement with available experimental results and theoretical values. With the aid of analysis of Λ–S composition of Ω states at different bond lengths, the avoided crossing phenomena in the electronic states of CS^+ are illuminated. Finally, the single ionization spectra of CS ($X^1\Sigma^+$) populating the CS^+($X^2\Sigma^+_{1/2}$, $A^2\Pi_{3/2}$, $A^2\Pi_{1/2}$, and $B^2\Sigma^+_{1/2}$) states are simulated. The vertical ionization potentials for $X^2\Sigma^+_{1/2}$, $A^2\Pi_{3/2}$, $A^2\Pi_{1/2}$, and $B^2\Sigma^+_{1/2}$ states are calculated to be 11.257, 12.787, 12.827, and 15.860 eV, respectively, which are accurate compared with previous experimental results, within an error margin of 0.08 eV∼0.2 eV.

Keywords: potential energy curves, spin–orbit coupling, carbon monosulfide molecular ion (CS^+), ionization spectrum

PACS: 31.50.Df, 31.15.aj, 31.15.ag **DOI:** 10.1088/1674-1056/22/12/123103

1. Introduction

Carbon monosulfide (CS) and its ion (CS^+) are an important molecule and molecular ion in astronomy, and have received much attention in spectroscopy[1–15] and astrophysics.[16–18] CS and CS^+ are usually formed in plasmas of sulfur and carbon using ultraviolet photolysis and the collisional dissociation of CS_2.[19] Since the dominant electronic configuration for the ground state of CS^+ ($6\sigma^2 2\pi^4 7\sigma^1$) has unpaired electrons, CS^+ is a short-lived and highly reactive diatomic molecular ion, and thus is usually treated as a radical. Due to the unstable nature and high density of the electronic states of CS^+, there are a series of complicated couplings among different electronic states, such as avoided crossing and spin–orbit coupling. Thus, assignment of electronic states and investigation of spectroscopic properties of CS^+ are of great potential importance for both experimental and theoretical studies.

As early as 1972, Frost *et al.*[1] observed CS^+ in a vacuum ultra-violet photoelectron spectrum of CS by means of He I radiation (He I PES). The ionization potentials (IPs) of $X^2\Sigma^+$ (11.34 eV), $A^2\Pi$ (12.78 eV), $B^2\Sigma^+$ (15.83 eV), $C^2\Sigma^+$ (18.03 eV), and spin–orbit splitting of $A^2\Pi$ (278 cm^{-1}) were obtained in their experiment. Since then, a series of spectroscopic studies has been carried out on the low-lying electronic states of CS^+. Tsuji *et al.*[2] detected the CS^+ ($B^2\Sigma^+$–$X^2\Sigma^+$) emission spectrum band produced by He (2^3S)/CS Penning ionization. Horani and Vervloet[18] measured the electronic spectrum of the $A^2\Pi$–$X^2\Sigma^+$ transition for CS^+ by employing Fourier transform spectroscopy. The (1, 0) absorption band,[6] (5, 0) and (6, 0) absorption bands,[8] and (2, 1) absorption band[12] of the $A^2\Pi$–$X^2\Sigma^+$ transition for CS^+ were observed through velocity modulation detection. Bailleux *et al.*[11] measured the submillimeter-wave spectrum of the ground state ($X^2\Sigma^+$) of CS^+ by employing positive column discharge in a CS_2–Ar mixture partially cooled by a limited flow of liquid nitrogen.

Along with experimental studies, numerous theoretical studies were also carried out to investigate the low-lying excited states for CS^+. In 1985, Larsson[3] computed potential energy curves (PECs) and spectroscopic parameters for the

*Project supported by the National Basic Research Program of China (973 Program) (Grant No. 2013CB922200), the National Natural Science Foundation of China (Grant Nos. 11034003, 11074095, and 11274140), the Natural Science Foundation of Heilongjiang Province, China (Grant No. QC2011C092), and the Scientific Research Fund of Heilongjiang Provincial Education Department, China (Grant No. 12531751).

†Corresponding author. E-mail: lirei01@163.com
‡Corresponding author. E-mail: yanbing@jlu.edu.cn

© 2013 Chinese Physical Society and IOP Publishing Ltd

$X^2\Sigma^+$, $A^2\Pi$, and $B^2\Sigma^+$ states of CS^+ by using complete active space SCF (CASSCF) and contracted configuration interaction (CI) methods. He also calculated non-orthogonal electronic transition moments between A–X, B–X, and B–A, and deduced the lifetimes of $A^2\Pi$ and $B^2\Sigma^+$ states. Later, Blöcker *et al.*[4] calculated electronic transition moment functions for the $A^2\Pi$–$X^2\Sigma^+$, $B^2\Sigma^+$–$X^2\Sigma^+$, $B^2\Sigma^+$–$A^2\Pi$, and $C^2\Delta$–$A^2\Pi$ transitions of CS^+ using highly correlated CASSCF CI methods, and evaluated the lifetimes of $A^2\Pi$, $B^2\Sigma^+$, and $C^2\Delta$ sates. Honjou[9] computed the PECs and spectroscopic constants for the $1\text{-}5^2\Sigma^+$ and $1\text{-}3^2\Pi$ states of CS^+ by employing *ab initio* CI methods. Subsequently, Honjou[10] calculated molecular vibrations of $X^2\Sigma^+$, $A^2\Pi$, $B^2\Sigma^+$, and $C^2\Sigma^+$ states of CS^+ using *ab initio* CI calculations, and simulated the photoelectron spectrum of CS. Liu *et al.*[13] calculated the PECs and spectroscopic properties for $X^2\Sigma^+$ and $A^2\Pi$ states of CS^+ using multi-reference CI methods. However, no theoretical studies including spin–orbit coupling (SOC) effects of the low-lying electronic states of CS^+ have been reported in previous literature. As is well known, the SOC effects play an important part in the spectrum and dynamics of the diatomic molecule, even if only the first-row and second-row atoms are included. Particularly, the SOC effects could lead to the state perturbation of different electronic states of CS^+. Thus, the avoided crossing phenomena of non-adiabatic PECs may occur between two different Λ–S states with the same Ω components due to the SOC effects.

In the present work, we use an *ab initio* method to calculate the PECs of low-lying electronic states of CS^+. In the PEC calculations, the SOC effects are taken into consideration via the state-interaction technique. Base on the calculated PECs, we further solve the nuclear Schrödinger equations to obtain vibrational energy levels, vibrational wave functions, and spectroscopic parameters of bound states for CS^+. Finally, the single ionization spectrum of CS is simulated.

2. Methods and computational details

In the present study, the *ab initio* calculations are performed with Molpro2010 suite of program package, designed by Werner *et al.*[20] All the calculations are performed in the C_{2v} subgroup of $C_{\infty v}$ and the corresponding relationships between the irreducible representations of the C_{2v} and $C_{\infty v}$ groups are $\Sigma^+ = A_1$, $\Pi = B_1 + B_2$, $\Delta = A_1 + A_2$, and $\Sigma^- = A_2$. In all the calculations, we describe the carbon atom with the contracted augmented correlation consistent polarized quintuple zeta Gaussian-type all-electron aug-cc-pwCV5Z basis set [15s, 9p, 5d, 4f, 3g, 2h],[21,22] and sulfur atom with the aug-cc-pwCV5Z basis set [21s, 13p, 5d, 4f, 3g, 2h].[22,23] The PECs of the low-lying doublet, quartet, and sextet electronic states of CS^+ are calculated with highly correlated *ab initio* methods, namely state-averaged complete active space self-consistent field (CASSCF) method[24,25] and the internally contracted multireference configuration interaction approach (MRCI) with Davison size-extensivity correction (+Q).[26–28] The selection of active space plays a vital role in the CASSCF computations, since the low-lying excited states arise from the excitation of valence electrons into the empty valence orbitals and the close-by outer-shell orbitals. Hence, the active space is comprised of 2p valence orbitals of C, 3s3p valence orbitals of S, and outer-shell $4s4p_x4p_y$ of S. In the subsequent calculations, the energies of 18 Λ–S states are calculated by MRCI + Q utilizing the CASSCF wave functions as reference wave function. In the above calculations, the scalar relativistic effects are taken into account through the second-order Douglas–Kroll[29] and Hess[30] one-electron integrals. The spin–orbit matrix elements and the spin–orbit eigenstates are computed by employing the state interaction method with the full Breit–Pauli Hamiltonian (H_{BP}).[31] In the SOC effect calculations, the $\hat{H}^{el}$ matrix elements are acquired from MRCI + Q computations, but the $\hat{H}^{SO}$ matrix elements are obtained from MRCI wave functions. The PECs are mapped by linking the energy points of electronic states considering the avoided crossing rule between the electronic states with the same Ω symmetry.

Based on the PECs of the bound Λ–S and Ω electronic states, the corresponding vibrational energy levels, vibrational wave functions, Franck–Condon factors (FCFs), and spectroscopic parameters are obtained from the numerical solution of nuclear Schrödinger equations by means of Le Roy's LEVEL procedure.[32]

3. Results and discussion

3.1. PECs of the low-lying Λ–S states

The 18 Λ–S states correlated to the two lowest dissociation limits $C(^3P) + S^+(^4S)$ and $C^+(^2P) + S(^3P)$ of CS^+ are calculated with the MRCI + Q method utilizing aug-cc-pwCV5Z basis set. The PECs for all the 18 Λ–S electronic states are shown in Fig. 1. For clarity, the doublet Λ–S states and the quartet/sextet Λ–S states are given in Figs. 1(a) and 1(b), respectively. For a series of given nuclear distances from $R = 1.2$ Å to $R = 3.7$ Å, each PEC is plotted by connecting 40 energy points of Λ–S electronic states. These PECs are depicted in energy relative to the minimum energy point of the ground state $X^2\Sigma^+$. As shown in Fig. 1, the PECs of $(3)^4\Pi$ and $(1)^6\Pi$ states are repulsive; the PECs of $(2)^2\Pi$, $(3)^2\Pi$, $(2)^2\Sigma^-$, and $(2)^4\Sigma^-$ exhibit double minima due to the avoided crossing phenomena between Λ–S states with the same symmetry

and spin multiplicity; the rest of the wcalculated Λ–S PECs are typically bound. The calculated spectroscopic constants of CS^+ are listed in Table 1, including adiabatic transition energies T_e, harmonic vibrational frequencies ω_e, anharmonic terms $\omega_e x_e$, rotational constants B_e, and equilibrium distance R_e. In Table 1 also listed are dominant electronic configurations of the 18 Λ–S electronic states at internuclear distance $R = 1.50$ Å. The spectroscopic constants obtained from previous experimental and theoretical studies are also listed in Table 1 for comparison. For the ground state $X^2\Sigma^+$, the calculated values of ω_e, $\omega_e x_e$, and B_e accord well with experimental data, each with an error of 5.883, 0.0195, and 0.0068 cm^{-1}, respectively; the difference between the latest experimental values[8] and our calculated ones of R_e is about 0.0059 Å. For $A^2\Pi$ and $B^2\Sigma^+$ states, the calculated spectroscopic constants T_e, ω_e, $\omega_e x_e$, B_e, and R_e are suitably consistent with the experimental results,[2,8,12] each with an error of 377.3 cm^{-1}, 1.173 cm^{-1}, 1.135 cm^{-1}, 0.0158 cm^{-1}, and 0.005 Å, respectively. Compared with previously calculated results,[3,9,10] the differences between experimental values and our calculated ones of the spectroscopic parameters of $X^2\Sigma^+$, $A^2\Pi$, and $B^2\Sigma^+$ states are evidently small. The above results indicate that the MRCI + Q PECs achieve good accuracy. In an energy range of $0 \sim 40000$ cm^{-1}, $A^2\Pi$ state crosses with $X^2\Sigma^+$ state, and $(1)^4\Pi$ state crosses with $X^2\Pi$, $(1)^4\Sigma^+$, $(1)^4\Delta$, and $B^2\Sigma^+$ states. When the spin–orbit coupling effects are taken into account, the state perturbation between these states may lead to the avoided crossing phenomena. For visual clarity, the PECs of $X^2\Sigma^+$, $A^2\Pi$, $(1)^4\Sigma^+$, $(1)^4\Delta$, $B^2\Sigma^+$, and $(1)^4\Pi$ states are plotted separately in Fig. 2. The ground state $X^1\Sigma^+$ of CS molecule is also computed with the MRCI + Q method using aug-cc-pwCV5Z basis set. The dominant electronic configuration of $X^1\Sigma^+$ is $6\sigma^2 2\pi^4 7\sigma^2$. From Table 1, it is found that the ground state $X^2\Sigma^+$ of CS^+ corresponds to the ejection of an electron from the outermost 7σ molecular orbital (MO) of CS. The dominant electron configuration of $A^2\Pi$ state originates from the removal of an electron from the 2π MO of CS. The dominant electron configurations of the following low-lying excited states: $(1)^4\Sigma^+$, $(1)^4\Delta$, and $B^2\Sigma^+$, correspond to the ejection of an electron from the outermost 7σ MO and simultaneous promotion of the second electron from 2π MO to vacant 3π MO. The dominant electronic configuration of $(1)^4\Pi$ ($6\sigma^2 2\pi^2 3\pi^1 7\sigma^2$) is described by the removal of an electron from the 2π MO and simultaneous promotion of the second electron from 2π MO to vacant 3π MO. As listed in Table 1, the equilibrium distance of $(1)^4\Pi$ (2.0227 Å) is much larger than those of other low-lying excited states including $(1)^4\Sigma^+$, $(1)^4\Delta$, and $B^2\Sigma^+$ because the 7σ MO is somewhat more nonbonding than the 2π MO.

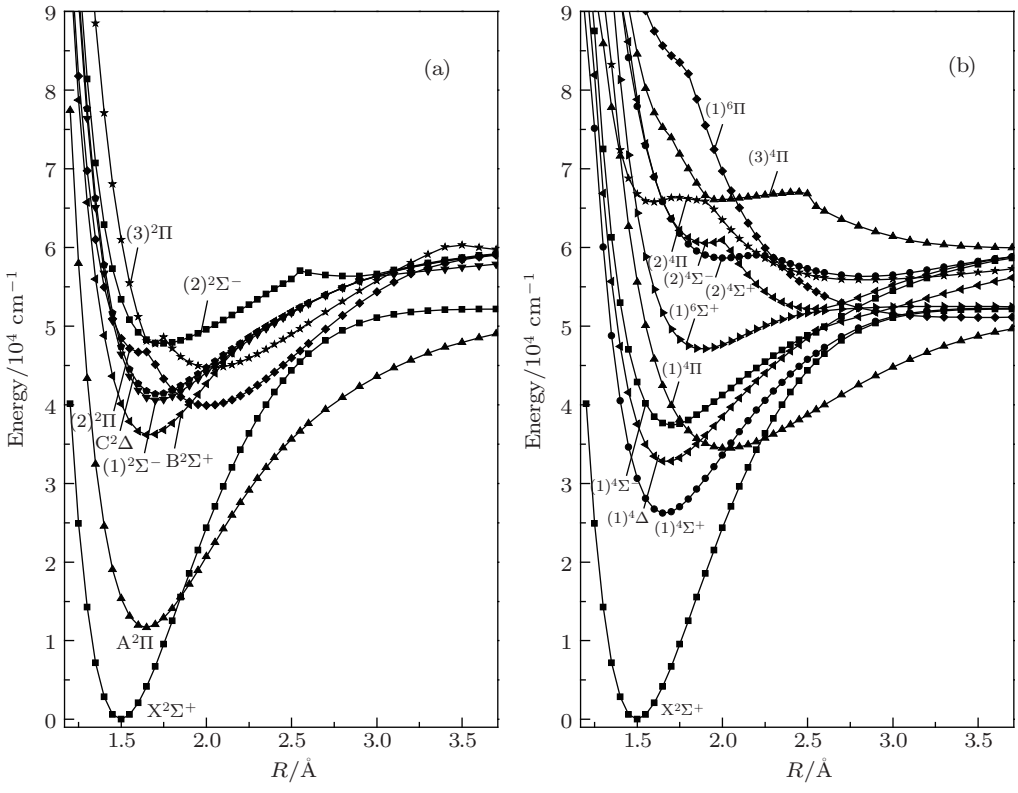


Fig. 1. Calculated MRCI + Q potential energy curves of CS^+ for (a) the doublet Λ–S states, and (b) the quartet/sextet Λ–S states. In each case, the ground state is given for comparison.

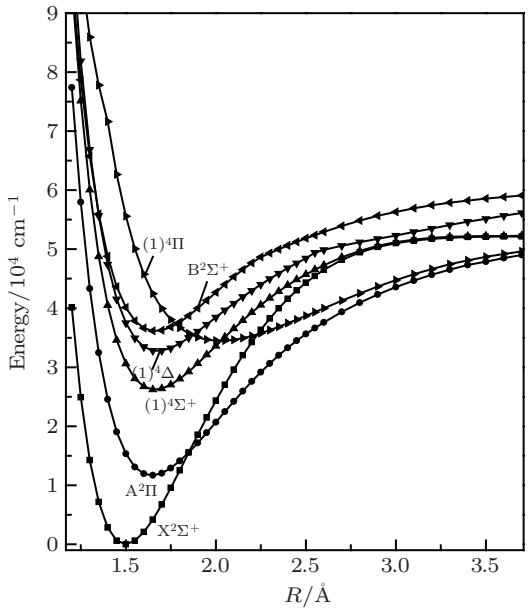


Fig. 2. (color online) Calculated MRCI + Q potential energy curves of $X^2\Sigma^+$, $A^2\Pi$, $(1)^4\Sigma^+$, $(1)^4\Delta$, $B^2\Sigma^+$, and $(1)^4\Pi$ states for CS^+.

As mentioned in the above section, the PECs of $(2)^2\Pi$ state exhibit a double-well potential. The values of T_e, ω_e, and R_e for $(2)^2\Pi$ state deduced from the outer potential well are 39900.9437 cm^{-1}, 554.0741 cm^{-1}, and 2.0033 Å. However, our calculated minimal value of the inner potential well of $(2)^2\Pi$ state appears at $R = 1.6288$ Å, which is smaller than that from another theoretical study, i.e., 1.685 Å.[9]

The different internuclear distances for local minimum of inner and outer potential wells could be attributed to the variation of the leading electronic configuration. Table 1 shows that the leading electronic configuration of $(2)^2\Pi$ is composed of $6\sigma^2 2\pi^4 3\pi^1$ (71%) at $R = 1.5$ Å; nevertheless, the electronic configuration of $(2)^2\Pi$ is mainly described by $6\sigma^2 2\pi^2 3\pi^1 7\sigma^2$ (81%) at $R = 2.0$ Å. In contrast to the 2π MO, the 7σ MO has nonbonding property, thus, the evolution of dominant electronic configuration of $(2)^2\Pi$ state along the internuclear distance leads to different local minimum positions for the double well of $(2)^2\Pi$. Finally, our work identifies the bound states $(1)^4\Sigma^+$, $(1)^4\Delta$, $(1)^4\Sigma^-$, $(1)^2\Sigma^-$, $C^2\Delta$, $(2)^2\Pi$, $(2)^2\Sigma^-$, $(1)^4\Pi$ $(1)^6\Sigma^+$, $(2)^4\Pi$, $(2)^4\Sigma^+$, and $(2)^4\Sigma^-$, which are previously uncharacterized either theoretically or experimentally.

Table 1. Computed and experimental spectroscopic constants of low-lying electronic states of CS^+.

State		T_e/cm^{-1}	ω_e/cm^{-1}	$\omega_e x_e$/cm^{-1}	B_e/cm^{-1}	R_e/Å	Configuration at $R = 1.50$ Å(%)
$X^2\Sigma^+$	This work	0	1371.6075	7.7925	0.8609	1.4981	$6\sigma^2 2\pi^4 7\sigma^1$(80) $6\sigma^2 2\pi^3 3\pi^1 7\sigma^1$(5)
	Expt.[a]		1384(30)				
	Expt.[b]	0	1377.49(16)	7.812(39)	0.867746 (91)	1.492156 (78)	
	Calc.[d]	0	1358.45	7.64	0.8575	1.501	
	Calc.[e]	0	1369			1.503	
	Calc.[f]	0	1357	7.6		1.503	
$A^2\Pi$	This work	11675.8809	1014.2091	6.5497	0.7143	1.6445	$6\sigma^2 2\pi^3 7\sigma^2$(89)
	Expt.[a]		972(30)				
	Expt.[b]	11987.25(67)	1013.90(37)	6.842(48)	0.718739 (90)	1.63955 (10)	
	Expt.[c]				0.7029211 (14)		
	Calc.[d]	11875.8	988.34	6.41	0.7074	1.653	
	Calc.[e]	11940	1004			1.650	
	Calc.[f]	12079	1001	7.8		1.650	
$(1)^4\Sigma^+$	This work	26204.6239	972.5645	7.8611	0.7004	1.6605	$6\sigma^2 2\pi^3 3\pi^1 7\sigma^1$(88)
$(1)^4\Delta$	This work	32730.6475	920.2092	10.7053	0.6896	1.6764	$6\sigma^2 2\pi^3 3\pi^1 7\sigma^1$(91)
$B^2\Sigma^+$	This work	36131.7388	912.1725	7.6352	0.6984	1.6642	$6\sigma^2 2\pi^3 3\pi^1 7\sigma^1$(58) $6\sigma^1 2\pi^4 7\sigma^2$(26)
	Expt.[a]		868(30)				
	Expt.[g]	36509	911(3)	6.5(1)		1.665	
	Expt.[b]						
	Calc.[d]	36993.5	920.6	6.44	0.6953	1.667	
	Calc.[e]	35980	907			1.670	
	Calc.[f]	35865	895	7.5		1.671	
$(1)^4\Sigma^-$	This work	37381.8917	804.4624	10.7117	0.6679	1.7010	$6\sigma^2 2\pi^3 3\pi^1 7\sigma^1$(91)
$(1)^2\Sigma^-$	This work	40569.8228	783.0202	10.1855	0.6595	1.7115	$6\sigma^2 2\pi^3 3\pi^1 7\sigma^1$(92)
$C^2\Delta$	This work	41332.1500	776.7235	10.9249	0.6577	1.7138	$6\sigma^2 2\pi^3 3\pi^1 7\sigma^1$(92)
$(2)^2\Pi$	This work	39900.9437	554.0741	1.7495	0.4814	2.0033	$6\sigma^2 2\pi^4 3\pi^1$(71) $6\sigma^1 2\pi^4 3\pi^1 7\sigma^1$(9)
$(2)^2\Sigma^-$	This work	47757.4481	589.8017	4.9367	0.6388	1.7353	$6\sigma^2 2\pi^3 3\pi^1 7\sigma^1$(89)
$(1)^4\Pi$	This work	34472.1167	504.9608	2.9397	0.4721	2.0227	$6\sigma^2 2\pi^2 3\pi^1 7\sigma^2$(88)
$(3)^2\Pi$	This work	44676.4760	475.3502	3.1518	0.4680	2.0312	$6\sigma^2 2\pi^2 3\pi^1 7\sigma^2$(87)
	Calc.[e]	48370	1497			1.685	
$(1)^6\Sigma^+$	This work	47086.0240	671.5008	18.7810	0.5459	1.8819	$6\sigma^2 2\pi^2 3\pi^2 7\sigma^1$(94)
$(2)^4\Pi$	This work	55868.0838	167.5973	0.6041	0.2425	2.8198	$6\sigma^1 2\pi^4 3\pi^1 7\sigma^1$(78) $6\sigma^2 2\pi^3 3\pi^2$(11)
$(2)^4\Sigma^+$	This work	56302.1006	248.6973	3.1229	0.2393	2.8424	$6\sigma^2 2\pi^2 3\pi^2 7\sigma^1$(86) $6\sigma^1 2\pi^3 3\pi^1 7\sigma^2$(7)
$(2)^4\Sigma^-$	This work	52170.1463	449.4983	6.2494	0.3009	2.5393	$6\sigma^2 2\pi^2 3\pi^2 7\sigma^1$(86) $6\sigma^1 2\pi^3 3\pi^1 7\sigma^2$(7)

Note: For the experimental values, the inaccuracy of measurement is depicted in the bracket.

[a]Ref. [1], [b]Ref. [8], [c]Ref. [12], [d]Ref. [3], [e]Ref. [9], [f]Ref. [10], [g]Ref. [2].

3.2. PECs of the low-lying Ω states

The next step in theoretical calculations is to take into account the SOC effects in the CS^+ molecular Hamiltonian. The Λ–S MRCI wave functions are used as a basis to solve the eigenequation of full Breit–Pauli Hamiltonian, and the resulting PECs are plotted by linking the calculated eigenvalues of the corresponding electronic state. All the Ω states obtained from 18 Λ–S states are computed, but only the 10 lowest Ω states generated from the 6 lowest Λ–S states in Fig. 2 are shown in Fig. 3 for the purpose of clarity. Based on the computed Ω-state PECs, the spectroscopic constants of CS^+ are evaluated numerically, which are listed in Table 2. In Table 3 are listed the Λ–S compositions of the Ω states at different internuclear distances. When taking into account the SOC effects, the recombination of electronic states with the same Ω symmetry will lead to the avoided crossing phenomena. There are four avoided crossing points located at $R = 1.85$ Å, $R = 1.9$ Å, $R = 2.05$ Å, and $R = 2.25$ Å, namely, Av-1, Av-2, Av-3, and Av-4, respectively, which are indicated by arrows in Fig. 3. As shown in Table 3, the leading composition of $X^2\Sigma^+$ state (the (1)1/2 state in Fig. 3(a)) changes from the $^2\Sigma^+$ state to $^2\Pi$ state at Av-1. Similarly, the predominant composition of $A^2\Sigma^+_{1/2}$ (the (5)1/2 state in Fig. 3(a)) varies from the $^2\Sigma^+$ state to $^4\Pi$ state at $R = 1.75$ Å, and from $^4\Pi$ state to $^4\Delta$ state at Av-2, which causes the (5)1/2 state to exhibit the double-well potential centered at $R = 1.6724$ Å and $R = 1.8624$ Å, respectively. The shallow well depths are 658 cm^{-1} and 988 cm^{-1}. The leading composition of $(1)^4\Delta_{1/2}$ (the (4)1/2 state in Fig. 3(a)) changes from $^4\Delta$ state to $^4\Pi$ state at Av-2, and from $^4\Pi$ state to $^2\Sigma^+$ state at Av-3, which results in the double-well potential of (4)1/2 state. Figure 3(a) shows that the double-well potential of (4)1/2 state is centered at $R = 1.6767$ Å and $R = 2.0$ Å, respectively, with the well depths being 2129 cm^{-1} and 395 cm^{-1}. The predominant composition of $(1)^4\Sigma^+_{1/2}$ (the (3)1/2 state in Fig. 3(a)) changes from $^4\Sigma^+$ state to $^4\Pi$ state at Av-3, and from $^4\Pi$ state to $^2\Sigma^+$ state at Av-4, which leads to a complex potential energy curve of the (3)1/2 state.

Table 2. Computed spectroscopic constants of low-lying states of CS^+.

State	T_e/cm^{-1}	ω_e/cm^{-1}	$\omega_e x_e$/cm^{-1}	B_e/cm^{-1}	R_e/Å
$X^2\Sigma^+_{1/2}$ (1)1/2	0	1371.0084	7.7725	0.8609	1.4981
$A^2\Pi_{3/2}$ (1)3/2	11542.4127	1020.0791	6.1290	0.7143	1.6444
$A^2\Pi_{1/2}$ (2)1/2	11811.9028	997.6023	–3.3075	0.7142	1.6444
$(1)^4\Sigma^+_{3/2}$ (2) 3/2	26200.8157	1136.3309	27.0050	0.7004	1.6605
$(1)^4\Sigma^+_{1/2}$ (3) 1/2	26204.9251	1132.5569	26.5573	0.7004	1.6605
$(1)^4\Delta_{1/2}$ (4) 1/2	32683.7730	765.3333	14.2032	0.6889	1.6767
$(1)^4\Delta_{3/2}$ (3) 3/2	32716.5669	764.3463	14.2635	0.6891	1.6764
$(1)^4\Delta_{5/2}$ (1) 5/2	32755.9639	735.1042	27.4263	0.6896	1.6762
$(1)^4\Delta_{7/2}$ (1) 7/2	32796.8918	925.6677	11.3729	0.6895	1.6757
$B^2\Sigma^+_{1/2}$ (5) 1/2	35611.8988	435.1411	–11.4172	0.5087	1.8624

From Fig. 3(b), it is also found that $(1)^4\Delta_{3/2}$ ((3)3/2) has two avoided crosses with $(1)^4\Pi_{3/2}$ state and $(1)^4\Sigma^+_{3/2}$ ((2)3/2) state at Av-2 and Av-3, respectively. The (3)3/2 state has a potential with double-wells of depths of 2064 cm^{-1} and 548 cm^{-1}. The doublet state $A^2\Pi$ and the quartet states $(1)^4\Sigma^+$ and $(1)^4\Delta$ each have spin–orbit splitting effect. The splitting energies of $A^2\Pi_{3/2}$–$A^2\Pi_{1/2}$, $(1)^4\Sigma^+_{3/2}$–$(1)^4\Sigma^+_{1/2}$, and $(1)^4\Delta_{1/2}$–$(1)^4\Delta_{7/2}$ are 269.4901, 4.1094, and 113.1188 cm^{-1}, respectively. The spin–orbit splitting of $A^2\Pi$ state (278 cm^{-1}) has been observed by Frost *et al.*[1] and accords well with our computed result.

Table 3. Composition of Ω states of CS^+ at different bond distances.

State	r/Å	$^2\Sigma^-$	$^2\Sigma^+$	$^2\Pi$	$^2\Delta$	$^4\Sigma^-$	$^4\Sigma^+$	$^4\Pi$	$^4\Delta$
$X^2\Sigma^+_{1/2}$	1.7		99.87						
	1.75		99.88						
	1.8		76.32	23.68					
	1.85			100					
	1.9			100					
	1.95			100					
	2.0			100					
	2.05			100					
$A^2\Pi_{1/2}$	1.7			100					
	1.75			100					
	1.8			100					
	1.85		23.68	76.32					
	1.9		100						
	1.95		100						
	2.0		100						
	2.05		100						
$A^2\Pi_{3/2}$	1.7			100					
	1.75			100					
	1.8			100					
	1.85			100					
	1.9			100					
	1.95			100					
	2.0			100					
	2.05			100					
$(1)^4\Sigma^+_{1/2}$	1.7						99.99		
	1.75						99.99		
	1.8						99.98		
	1.85						99.97		
	1.9						99.94		
	1.95						99.86		
	2.0						8	91.96	
	2.05							99.94	
	2.2							99.93	
	2.25		99.80					0.2	
$(1)^4\Sigma^+_{3/2}$	1.7					99.94			
	1.75					99.94			
	1.8					99.93			
	1.85					99.93			
	1.9					99.91			
	1.95					99.86			
	2.0					98.89			
	2.05					0.92		98.98	

Table 3. (*Continued*)

State	r/Å	$^2\Sigma^-$	$^2\Sigma^+$	$^2\Pi$	$^2\Delta$	$^4\Sigma^-$	$^4\Sigma^+$	$^4\Pi$	$^4\Delta$
$(1)^4\Delta_{1/2}$	1.7								100
	1.75								99.99
	1.8								99.99
	1.85								99.95
	1.9							99.9	
	1.95							99.9	
	2.0							99.74	
	2.05					97.84		1.05	
$(1)^4\Delta_{3/2}$	1.7								100
	1.75								99.99
	1.8								99.99
	1.85								99.95
	1.9							99.9	
	1.95							99.9	
	2.0							99.74	
	2.05						98.91		
$(1)^4\Delta_{5/2}$	1.7								100
	1.75								99.99
	1.8								99.99
	1.85								99.95
	1.9							99.9	
	1.95							99.9	
	2.0							99.9	
	2.05							99.9	
$(1)^4\Delta_{7/2}$	1.7								100
	1.75								100
	1.8								100
	1.85								100
	1.9								100
	1.95								100
	2.0								100
	2.05								100
$B^2\Sigma^+_{1/2}$	1.7		99.66						
	1.75		98.34			1.07		0.54	
	1.8							98.94	
	1.85							98.94	
	1.9								99.95
	1.95								99.95
	2.0								99.93
	2.05			0.12					99.88
	2.1			99.86					

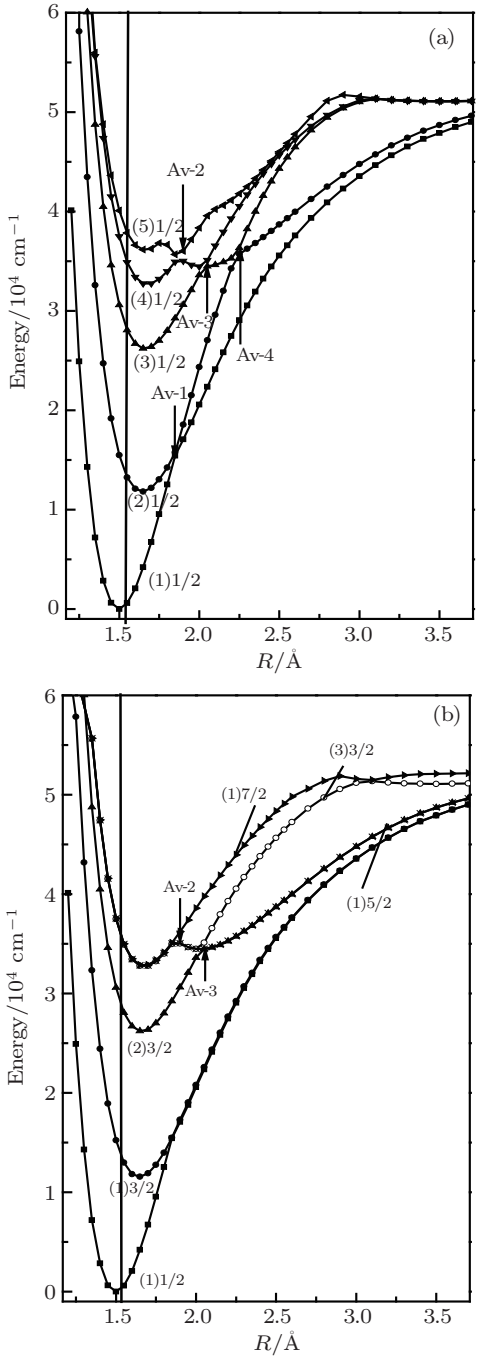


Fig. 3. Potential energy curves with the spin–orbit coupling effects of the low-lying electronic state of CS^+ for (a) $\Omega = 1/2$, (b) $\Omega = 3/2$, $\Omega = 5/2$, and $\Omega = 7/2$ states, respectively. The vertical line is correlated to the middle of the Franck-Condon region, that is, the maximum of the CS ($X^1\Sigma^+$, $v = 0$) wave function.

3.3. Theoretical single ionization spectra of CS

As is well known, the photoelectron spectrum (PES) of a molecule arising from the direct ionization of the molecule can be simulated by the FCFs of direct ionization transition between the ground state of the molecule and the corresponding electronic state of the molecular ion. Thus, we calculate the FCFs for ionization transition between the electronic states ($X^2\Sigma^+_{1/2}$, $A^2\Pi_{1/2}$, and $A^2\Pi_{3/2}$) of CS^+ and the ground state ($X^1\Sigma^+$) of CS. In the calculations, we adopt "Q-branch" approximation, meaning that only the $\Delta J = 0$ transitions are included. Then, the singlet ionization spectra of CS are fitted with a Gaussian function utilizing a conventional resolution of 10 meV. The corresponding ionization spectra are shown in Fig. 4. The horizontal axis shows the ionization energy from the vibrational ground state of CS ($X^1\Sigma^+$). Based on the potential energy curves of CS/CS^+ calculated with the aug-cc-pwCV5Z/MRCI + Q method including spin–orbital coupling effects, the vertical IP for $X^2\Sigma^+_{1/2}$ is calcu-

lated to be 11.257 eV, which accords well with the experimental result of 11.34 eV.[1] Figure 4 shows that there are three bands in the energy range of 11 eV–16.5 eV. The first band arises from CS^+ ($X^2\Sigma^+_{1/2}$, v^+) + e^- ← CS ($X^1\Sigma^+, v = 0$) + $h\nu$ transitions. The second band stems from CS^+ ($A^2\Pi_{3/2}$, v^+) + e^- ← CS ($X^1\Sigma^+, v = 0$) + $h\nu$, and CS^+ ($A^2\Pi_{1/2}, v^+$) + e^- ← CS ($X^1\Sigma^+, v = 0$) + hν transitions. The third band is ascribed to CS^+ ($B^2\Sigma^+_{1/2}, v^+$) + e^- ← CS ($X^1\Sigma^+$, v = 0) + $h\nu$ transitions. The vertical IPs for $A^2\Pi_{3/2}$, $A^2\Pi_{1/2}$, and $B^2\Sigma^+_{1/2}$ states are calculated to be 12.787, 12.827, and 15.860 eV, respectively, which are very close to the experimental results, i.e., 12.90, 12.90, and 16.06 eV.[1] Our calculated adiabatic IPs for $A^2\Pi_{3/2}$, $A^2\Pi_{1/2}$, and $B^2\Sigma^+_{1/2}$ states are 12.662, 12.695, and 15.709 eV, respectively, which are in excellent agreement with experimental values, i.e., 12.78, 12.78, and 15.83 eV.[1] As discussed in Subsection 3.2, the calculated spin–orbit splitting energy of $A^2\Pi_i$ is suitably consistent with the experimental result,[1] with an error of less than 8 cm^{-1}. Due to the different equilibrium internuclear distances between the ground state of CS and electronic state of CS^+, a relatively long vibrational progression is observed in the simulated spectrum. From Fig. 4, it is found that the FCFs of $X^2\Sigma^+$ ←$X^1\Sigma^+$ transitions are significantly larger than those of $A^2\Pi_i$ ←$X^1\Sigma^+$ transitions. Since the equilibrium bond distance of CS^+ ($X^2\Sigma^+$) state is located in the middle of the Franck–Condon region of the ground state of neutral CS, the vibrational transitions in CS^+ ($X^2\Sigma^+$) ← CS ($X^1\Sigma^+$) process are favorable due to large Franck–Condon overlap of corresponding wave functions.

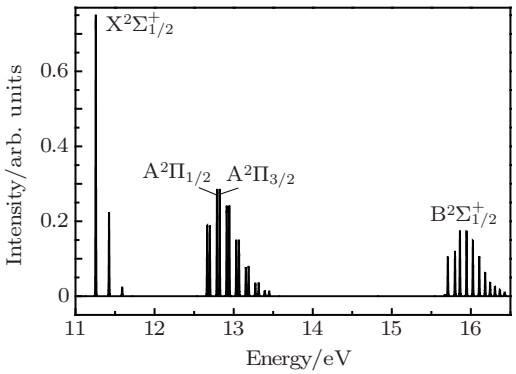


Fig. 4. Simulation of the single ionization spectra of CS using Gaussian function with an FWHM of 10 meV.

4. Conclusions

The potential energy curves of the ground and low-lying excited states for CS^+ molecular ion are investigated by employing the MRCI + Q method (including the Douglas–Kroll scalar relativistic correction) with all-electronic aug-cc-pwCV5Z basis set. The potential energy curves of the 18 Λ–S states correlated with the two lowest dissociation limits and the 10 lowest Ω states generated from the 6 lowest Λ–S states are obtained, from which the spectroscopic constants are evaluated. Our calculated values are in good accordance with existing experimental and theoretical results. From the potential energy curves of 18 Λ–S states, it is found that $A^2\Pi$ state crosses with $X^2\Sigma^+$ state, and $(1)^4\Pi$ state crosses with $X^2\Pi$, $(1)^4\Sigma^+$, $(1)^4\Delta$, and $B^2\Sigma^+$ states in an energy range of $0 \sim 40000$ cm^{-1}. With the aid of analysis of Λ–S composition of Ω states at different bond lengths, the interactions between these crossing states are explained, illuminating the avoided crossing phenomena of these states. Our theoretical investigation indicates that the spin–orbit coupling plays an important role in the low-lying excited states for CS^+ molecular ion, and makes the potential energy curves of Ω states more complicated. Finally, the single-ionization spectra from CS ($X^1\Sigma^+$ state) to CS^+ ($X^2\Sigma^+$, $A^2\Pi_{3/2}$, $A^2\Pi_{1/2}$, and $B^2\Sigma^+$ states) are simulated. The computed vertical adiabatic IPs of CS are highly consistent with experimental results. The present theoretical study may add some understanding to and shed more light on the structure and spectroscopic properties of the low-lying electronic states of CS^+ molecular ion.

References

[1] Frost D C, Lee S T and McDowell C A 1972 *Chem. Phys. Lett.* **17** 153

[2] Tsuji M, Obase H and Nishimura Y 1980 *J. Chem. Phys.* **73** 2575

[3] Larsson M 1985 *Chem. Phys. Lett.* **117** 331

[4] Blöcker J H, Reinsch E A, Rosmus P, Werner H J and Knowles P J 1990 *Chem. Phys.* **147** 99

[5] Dyke J M, Gamblin S D, Haggerston D, Morris A, Stranges S, West J B, Wright T G and Wright A E 1998 *J. Chem. Phys.* **108** 6258

[6] Liu Y, Liu H, Gao H, Duan C, Hamilton P A and Davies P B 2000 *Chem. Phys. Lett.* **317** 181

[7] Barr J D, Beeching L, De Fanis A, Dyke J M, Gamblin S D, Hooper N, Morris A, Stranges S, West J B, Wright A E and Wright T G 2000 *J. Electron Spectrosc.* **108** 47

[8] Liu Y, Duan C, Liu J, Wu L, Xu C, Chen Y, Hamilton P A and Davies P B 2002 *J. Chem. Phys.* **116** 9768

[9] Honjou N 2006 *Chem. Phys.* **324** 413

[10] Honjou N 2008 *Chem. Phys.* **344** 128

[11] Bailleux S, Walters A, Grigorova E and Margulès L 2008 *Astrophys. J.* **679** 920

[12] Li C, Deng L, Zhang Y, Yang X and Chen Y 2010 *J. Mol. Spectrosc.* **264** 75

[13] Liu H, Xing W, Shi D H, Zhu Z L and Sun J F 2011 *Acta Phys. Sin.* **60** 043102 (in Chinese)

[14] Yan B and Zhang Y J 2013 *Chin. Phys. B* **22** 023103

[15] Li R, Wei C L, Sun Q X, Sun E P, Xu H F and Yan B 2013 *J. Phys. Chem. A* **117** 2373

[16] Ferlet R, Roueff E, Czarny J and Felenbok P 1986 *Astron. Astrophys.* **168** 259

[17] Drdla K, Knapp G R and van Dishoeck E F 1989 *Astrophys. J.* **345** 815

[18] Horani M and Vervloet M 1992 *Astron. Astrophys.* **256** 683

[19] Zhang W, Xie T, Huang Y, Wang G R and Cong S L 2013 *Chin. Phys. B* **22** 013301

[20] Werner H J, Knowles P J, Knizia G, Manby F R, Schütz M, Celani P, Korona T, Lindh R, Mitrushenkov A, Rauhut G, Shamasundar K R, Adler T B, Amos R D, Bernhardsson A, Berning A, Cooper D L, Deegan M J O, Dobbyn A J, Eckert F, Goll E, Hampel C, Hesselmann A, Hetzer G, Hrenar T, Jansen G, Köppl C, Liu Y, Lloyd A W, Mata R A, May A J, McNicholas S J, Meyer W, Mura M E, Nicklass A, Neill D P, Palmieri P, Peng D, Pflüger K, Pitzer R, Reiher M, Shiozaki T, Stoll H, Stone A J, Tarroni R, Thorsteinsson T and Wang M 2010 MOLPRO: A Package of *ab initio* Programs

[21] Kendall R A, Dunning T H and Harrison R J 1992 *J. Chem. Phys.* **96** 6796

[22] Peterson K A and Dunning T H 2002 *J. Chem. Phys.* **117** 10548

[23] Woon D E and Dunning T H 1993 *J. Chem. Phys.* **98** 1358

[24] Knowles P J and Werner H J 1985 *Chem. Phys. Lett.* **115** 259

[25] Werner H and Knowles P J 1985 *J. Chem. Phys.* **82** 5053

[26] Langhoff S R and Davidson E R 1974 *Int. J. Quantum Chem.* **8** 61

[27] Knowles P J and Werner H J 1988 *Chem. Phys. Lett.* **145** 514

[28] Werner H J and Knowles P J 1988 *J. Chem. Phys.* **89** 5803

[29] Douglas M and Kroll N M 1974 *Ann. Phys.* **82** 89

[30] Hess B A 1986 *Phys. Rev. A* **33** 3742

[31] Berning A, Schweizer M, Werner H J, Knowles P J and Palmieri P 2000 *Mol. Phys.* **98** 1823

[32] Le Roy R J 2002 LEVEL 7.5: a Computer Program for Solving the Radial Schröinger Equation for Bound and Quasibound Levels (University of Waterloo, Chemical Physics Research Report CP-655)